

# Vascular imaging with contrast agent in hard and soft tissues using microcomputed-tomography

P. BLERY\*, †, P. PILET\*, A. VANDEN-BOSSCHE‡, A. THERY\*, §, J. GUICHEUX\*, Y. AMOURIQ\*, †, F. ESPITALIER\*, §, N. MATHIEU|| & P. WEISS\*, †

\*Inserm U791, LIOAD, Faculté de Chirurgie Dentaire, 1 Place Alexis Ricordeau, 44042 Nantes Cedex 1, France

†Faculté de chirurgie dentaire, Université de Nantes, 1 Place Alexis Ricordeau, 44042 Nantes Cedex 1, France

‡Inserm U1059, Laboratoire de Biologie intégrative du Tissu Osseux, Faculté de Médecine, 15 rue Ambroise Paré, 42023 Saint-Etienne cedex

§Service d'ORL et de chirurgie cervico-faciale, CHU Hôtel Dieu, 1 place Alexis Ricordeau, 44042 Nantes Cedex 1, France

||IRSN Institut de Radioprotection et de Sécurité Nucléaire, IRSN/PRP-HOM/SRBE/LR2I, 31 avenue de la division Leclerc BP17, 92260 Fontenay aux roses, France

**Key words.** Barium sulphate, contrast agent, imaging, micro-CT, vascularization.

## Summary

Vascularization is essential for many tissues and is a main requisite for various tissue-engineering strategies. Different techniques are used for highlighting vasculature, *in vivo* and *ex vivo*, in 2-D or 3-D including histological staining, immunohistochemistry, radiography, angiography, microscopy, computed tomography (CT) or micro-CT, both stand-alone and synchrotron system. Vascularization can be studied with or without a contrast agent. This paper presents the results obtained with the latest Skyscan micro-CT (Skyscan 1272, Bruker, Belgium) following barium sulphate injection replacing the bloodstream in comparison with results obtained with a Skyscan In Vivo 1076. Different hard and soft tissues were perfused with contrast agent and were harvested. Samples were analysed using both forms of micro-CT, and improved results were shown using this new micro-CT. This study highlights the vasculature using micro-CT methods. The results obtained with the Skyscan 1272 are clearly defined compared to results obtained with Skyscan 1076. In particular, this instrument highlights the high number of small vessels, which were not seen before at lower resolution. This new micro-CT opens broader possibilities in detection and characterization of the 3-D vascular tree to assess vascular tissue engineering strategies.

## Introduction

Vascularization is essential for all cells and organs as well as the soft and hard tissues of the body. It plays a vital role in tissue development, breathing and circulation. Many diseases

involve a defect in the vascular network, making research into vascularization an important aspect within tissue engineering understanding and stimulating interaction between angiogenic and osteogenic pathways (Carano & Filvaroff, 2003; Saran *et al.*, 2014). However, to assess the involvement of vasculature in pathological processes or to measure the benefit of therapeutic strategies, the vascular network must be precisely and reproductively quantified and visualized. Different techniques can be used to observe vasculature, such as histological staining or imaging (Grabherr *et al.*, 2007; Jia *et al.*, 2010; Pabst *et al.*, 2014). Histological staining (e.g. Hematoxylin-Eosin, Movat pentachrome; or CD31 and vWF immunohistochemistry) may be used to see the relationship between vessels and the surrounding structures and tissues. Different direct imaging techniques are possible, such as radiography, angiography, microscopy, computed tomography (CT) and micro-CT. In imaging studies, a contrast agent is often used to highlight the vessels. Many contrast agents can be used: iodine, liquid fatty oil, resin, gold nanoparticles and the two most commonly used Microfil<sup>®</sup> and barium sulphate (Duvall *et al.*, 2004; Marxen *et al.*, 2004; Grabherr *et al.*, 2007; Young *et al.*, 2008; Mondy *et al.*, 2009a, 2009b; Schneider *et al.*, 2009; Chien *et al.*, 2010; Hallouard *et al.*, 2010; Jia *et al.*, 2010; Langer *et al.*, 2011; Nyangoga *et al.*, 2011; Pabst *et al.*, 2014; Roche *et al.*, 2012). We have made a lot of tests using these two contrast agents. Barium sulphate has been demonstrated to give better results as in the literature (Jia *et al.*, 2010; Prisby *et al.*, 2011; Roche *et al.*, 2012, 2013) and was used in this study. Indeed, Microfil showed rounded artefacts, seems to change vascular anatomy and using it also need to decalcify the samples for study them by micro-CT. Different samples, from hard (mandibles and long bones) to soft tissues (heart, kidney . . .), were harvested and acquired with two micro-CT: an In Vivo Skyscan 1076 and the new generation of micro-CT,

Correspondence to: Pauline Blery, INSERM U791 LIOAD—Faculté de Chirurgie Dentaire, 1 place Alexis Ricordeau, 44042 Nantes Cedex 1. Tel: 0240412917; fax: 0240083712; e-mail: pauline.blery@univ-nantes.fr

**Table 1.** Micro CT acquisition parameters with Skyscan 1272 for different samples.

	Resolution in $\mu\text{m}$	Voltage in kV	Amperage in $\mu\text{A}$	Filter	Rotation step in $^\circ$	Rotation sample in $^\circ$	Image size in pixels (Width*Height)
Head	6	100	100	Al 0.5 mm	0.30 $^\circ$	180 $^\circ$	3840*3840
Mandible	6	90	111	Al 0.5 mm	0.45 $^\circ$	180 $^\circ$	3840*3840
Front legs	6	60	140	Al 0.5 mm	0.45 $^\circ$	180 $^\circ$	5664*5664
Larynx	3	50	100	Al 0.25 mm	0.30 $^\circ$	180 $^\circ$	4032*4032
Heart	6	60	100	Al 0.25 mm	0.45 $^\circ$	180 $^\circ$	2016*2016
Lungs	5	100	100	Cu 0.11 mm	0.45 $^\circ$	180 $^\circ$	5664*5664
Kidneys	6	100	100	Al 0.5 mm	0.45 $^\circ$	180 $^\circ$	2016*2016
Liver	5	60	140	Al 0.5 mm	0.45 $^\circ$	180 $^\circ$	5664*5664
Spleen	6	60	100	Al 0.25 mm	0.45 $^\circ$	180 $^\circ$	2016*2016
Femurs	6	100	100	Al 0.5 mm	0.45 $^\circ$	180 $^\circ$	2016*2016
Tibiae	6	100	100	Al 0.5 mm	0.45 $^\circ$	180 $^\circ$	2016*2016
Back legs	4	100	100	Al 0.5 mm	0.30 $^\circ$	180 $^\circ$	4032*4032

**Table 2.** Parameters of acquisition and reconstruction of tibia and mandible after SIV1076 and S1272 micro-CT acquisition.

Bones studied	Tibia		Mandible	
	Skyscan In Vivo 1076	Skyscan 1272	Skyscan In Vivo 1076	Skyscan 1272
Micro-CT				
Voltage	70 kV	70 kV	70 kV	90 kV
Amperage	141 $\mu\text{A}$	141 $\mu\text{A}$	141 $\mu\text{A}$	111 $\mu\text{A}$
Rotation step	0,7 $^\circ$	0,7 $^\circ$	0,7 $^\circ$	0,45 $^\circ$
Pixel Size	9 $\mu\text{m}$	9 $\mu\text{m}$	9 $\mu\text{m}$	6 $\mu\text{m}$
Projection format	TIFF 16 bits	TIFF 16 bits	TIFF 16 bits	TIFF 16 bits
Number of projections	568	1104	568	2502
Image size Rows*Columns	2672*2000	1344*2016	2672*4000	1337*3840
Reconstruction format	BMP 8 bits	BMP 8 bits	BMP 8 bits	BMP 8 bits
Number of slices	3950	4056	3815	5080
Image size Width*Height	2000*2000	2016*2016	4000*4000	3840*3840

**Table 3.** Micro-CT characteristics (from the vendor).

Skyscan In VIVO 1076 (SIV 1076)	Skyscan 1272 (S 1272)
11 Mp X-ray camera	11 Mp X-ray camera
Voltage: 90 kV	Voltage: 140 kV
8000*8000 Pixels in every slice	8000*8000 Pixels in every slice
Resolution: Down to 9 $\mu\text{m}$	Resolution: Down to 0.7 $\mu\text{m}$
Integrated physiological monitoring	

the Skyscan 1272. This study sought to find the best way to visualize the vasculature and show vasculature highlighted by micro-CT systems after contrast agent injection. The final aim was to detect and characterize the 3-D vascular tree in order to quantify the benefits for vascularization in vascular engineering strategies.

## Materials and methods

The contrast agent was prepared by mixing 50% barium sulphate (Micropaque<sup>®</sup>, Guerbet, France) in PBS (phosphate buffer saline, Sigma-Aldrich, Saint-Quentin Fallavier, France)

with 1.5% of gelatin. PBS was heated to 90 $^\circ\text{C}$  in order to melt the gelatin and obtain a clear mixture. Warmed barium sulphate was added slowly and allowed to mix to obtain a homogeneous solution. Following cooling, the barium sulphate mixture was preserved at 4 $^\circ\text{C}$ .

All experiments were conducted in compliance with French laws and guidelines for animal experiments (Act no.92–333, 2 October 2009) and approved by the Ethics Committee of Animal Experimentation CEEA number 810 (Protocol numbers: P07–15 and P14–2). Three hundred gram wild-type male Sprague-Dawley rats were purchased from Charles River Laboratories (France). The animals were housed in double-decker cages, three to a cage, with full access to food and water and submitted to light and dark cycles.

Rats were anesthetized with isoflurane. The animal's thorax was disinfected and then the abdominal cavity and thorax were opened. A catheter was fixed in the left ventricle of the heart and was maintained with a touch of glue (cyanoacrylate). The second end of the catheter was connected in barium sulphate mixture warmed at 40 $^\circ\text{C}$ . The right atrium was sectioned and the injection was started. Approximately 200 mL

of contrast agent was injected into the bloodstream with a peristaltic pump at a regular flow ( $750 \text{ mL h}^{-1}$ ) until the animal's extremities became white. The animals died during the injection under anaesthesia. After perfusion of all the vasculature, samples were harvested and fixed in 4% PFA.

Initially, a few samples were imaged using micro-CT with an In Vivo Skyscan 1076 (Skyscan, Bruker, Belgium) at a pixel size of  $9 \mu\text{m}$  (70kV/140  $\mu\text{A}$ ; rotation step at  $0.7^\circ$  on  $180^\circ$  (257 projections;  $180^\circ$  was chosen rather than  $360^\circ$  to decrease acquisition time); time exposure 1.2 s; 0.5 mm aluminium filter, image size 4000\*4000).

Samples were then imaged with a Skyscan 1272 (Skyscan, Bruker, Belgium). Mineralized samples or organs and soft tissues were harvested and imaged in plastic tubes containing 70% alcohol. Acquisition parameters were chosen according to the samples: pixel size between 3, 6 and  $9 \mu\text{m}$ ; rotation step  $0.3^\circ$ - $0.45^\circ$ - $0.7^\circ$  (600 or 400 projections), always on  $180^\circ$ , filter chosen between aluminium 0.5 mm to copper 0.11 mm (according to the degree of X-ray absorbance by the structure), with an image size approximately 2016\*2016, 3840\*3840, 4032\*4032 or 5664\*5664 (depending on the sample's sizes; Tables 1–3).

NRecon Reconstruction Software (using Feldkamp algorithm) was used for reconstruction and then CtVox software for 3-D imaging (Skyscan, Bruker, Belgium). The micro-CT characteristics (from the vendor) are presented in Table 3, called SIV for Skyscan In Vivo 1076 and S1272 for Skyscan 1272.

## Results

Contrast agent preparation and injection occurred adequately to enable micro-CT images. Approximately 200 mL of contrast agent was injected allowing the visualization of all the organs, soft tissues and probably the bones (the perfusion of bones cannot be controlled during experiments).

First, the head, mandible and femurs were harvested and imaged with both micro-CT machines (SIV1076 at  $9 \mu\text{m}$  and S1272 at 6 or  $9 \mu\text{m}$ ). A qualitative observation shows differences between the images obtained by both micro-CT devices.

For hard tissues, including bone, a greater number of vessels were detected. With the SIV1076, the contours of vessels and bone were blurred and the vessels appeared thickened (Figs. 1 and 2). With the S1272, many more vessels were visible and much sharper; the trabecular aspect of bone was clearly shown. Bone and vessels were distinguished more easily. Differences were observed when comparing 3-D volumes as well as 2-D slices, also at the same resolution. Histograms, of the grey levels of the raw CT slices, were similar after using the two micro-CT systems (Figs. 1 and 2).

In soft tissues, the results were equally improved. The contrast of the vessels with bone was also sharper. For the mandible images, numerous vessels of soft tissues surrounding the mandibles took up contrast agent very well and were

visible with the new machine (Fig. 3). For the head, the vessels could be tracked or followed, as could the connections and divisions of the vessels; all the vessels were perfused and no gaps could be observed (Fig. 4). The microvascularization of the tongue was readily visible with this new micro-CT compared to the old one where only large trunks were visible; also, vascularization of the dental pulp was visible.

Many vessels were more visible and much more accurately and clearly defined using the S1272. Almost the entire vascular tree was visible and the number of artefacts and gaps was substantially reduced with the S1272 due to the improvement of the camera and the X-ray source. The smallest vessels, which were clearly delineated with the SIV1076, were about  $8 \mu\text{m}$  whereas with the S1272, the smallest vessel diameter visible is around 2 or  $3 \mu\text{m}$  (measured with the CtAn software; Figs. 1–4).

Different organs and soft or hard tissues were harvested for only the S1272 micro-CT analysis. Organs came from different rats, but the same strain was used; a mandible with the tongue on left and a liver on right (Fig. 5); a lung on left and a kidney on right (Fig. 6); all the vascular network was perfused even the smallest vessels.

The used filter as well as the voltage and amperage were selected according to samples in order to see vessels and organ structures. In addition, the files were much larger at this resolution (e.g. acquisition files of a mandible with the SIV1076 were around 10 GB, reconstruction files around 30 GB; with the S1272 acquisition files were 30 GB and reconstruction files around 70 GB). For reconstruction and 3-D volume construction, a powerful computer is required or a cluster of computers [we used a DELL Precision 7610 with two Intel Xeon CPU E5 2680V2 processors, 2.8 GHz, 128 GB RAM, and two graphic cards (Nvidia quadro K5000, Nvidia tesla K20C)].

However, the images obtained with the S1272 seem to be an improvement because close to the entire vascular tree was visible for the soft tissues. Three-dimensional volume images (organs were harvested and imaged separately) and were merged to recreate a whole animal and are presented in Figure 7.

For soft tissues, using S1272, the qualitative results were much better. However, differences can be observed for bone between samples. Although contrast agent was injected uniformly, acquisition parameters were the same, the results of bone perfusion are not perfectly identical, probably due to the considerable heterogeneity between individuals' bone vascular network.

## Discussion

Vascularization plays a crucial role in survival (Carano & Filvaroff, 2003; Saran *et al.*, 2014). Different techniques can be used to evidence the vasculature, based on imaging or combined with histological staining (Pabst *et al.*, 2014). Our study attempted to determine an injection protocol that was both reliable and reproducible and a good technique to

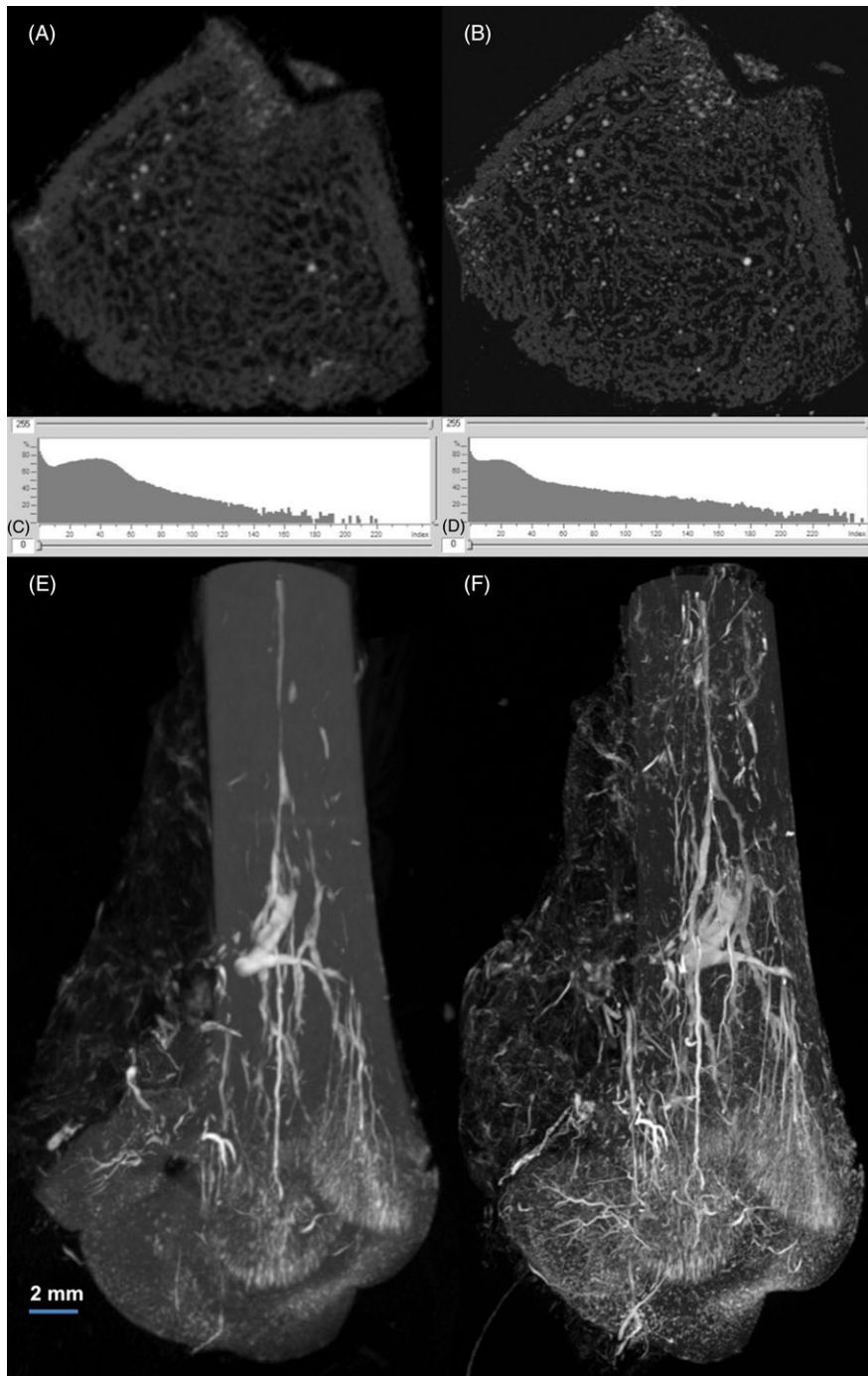


**Fig. 1.** Slices of femur (A and B) and 3-D femur volumes (E and F) after barium sulphate injection and acquisition with two micro-CT devices: the SIV1076 on the left (A and E) at  $9\ \mu\text{m}$  and the S1272 at  $6\ \mu\text{m}$  on the right (B and F) (2016\*2016). Histograms of grey levels of raw CT slices, at (C and D).

highlight this vasculature. Different contrast agents and injection protocols have been detailed in the literature (Grabherr *et al.*, 2007; Young *et al.*, 2008). The most commonly used contrast agents are Microfil<sup>®</sup> and barium sulphate. Microfil<sup>®</sup> is a silicon containing lead chromate that perfuse well into the soft tissues, but contrast agent and bone have the same X-ray

absorbance and consequently the same grey level. This is a disadvantage when studying bone and requires bone decalcification when using this contrast agent (Bentley *et al.*, 2002; Duvall *et al.*, 2004; Marxen *et al.*, 2004; Bolland *et al.*, 2008; Young *et al.*, 2008; Mondy *et al.*, 2009a, 2009bb; Nyangoga *et al.*, 2011; Roche *et al.*, 2012). We therefore chose barium

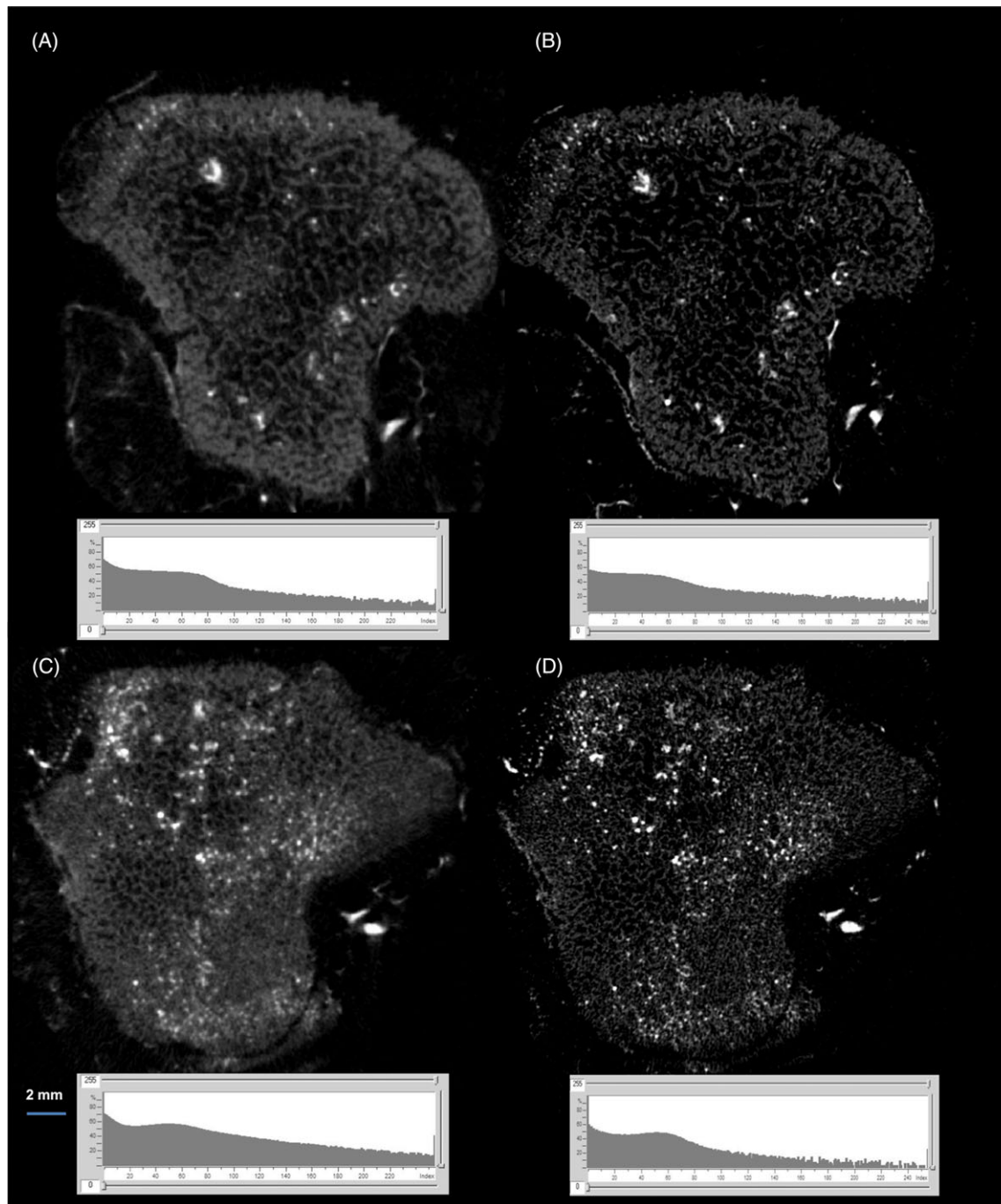


**Fig. 2.** Slices of the same tibia, at two different locations, after barium sulphate injection and acquisition at  $9\ \mu\text{m}$  with two micro-CT devices: the SIV1076 on the left (A and C) and the S1272 on the right (B and D), with each histogram of grey levels.

sulphate for this study as recommended by a number of authors (Moore *et al.*, 2003; Duvall *et al.*, 2004; Marxen *et al.*, 2004; Oses *et al.*, 2009; Schneider *et al.*, 2009; Jia *et al.*, 2010; Roche *et al.*, 2012). We tested many mixtures, with different gelatin or barium sulphate percentages; the results were irrelevant or could not be reproduced. However, the best results

were found after the perfusion technique in the heart, using a warmed mixture of barium sulphate with a peristaltic pump (Jia *et al.*, 2010; Roche *et al.*, 2012, 2013). To visualize the vascular tree, different techniques can be used: histological staining, immunohistochemistry, scanning electron microscopy and micro-CT (Pabst *et al.*, 2014). The use of micro-CT to

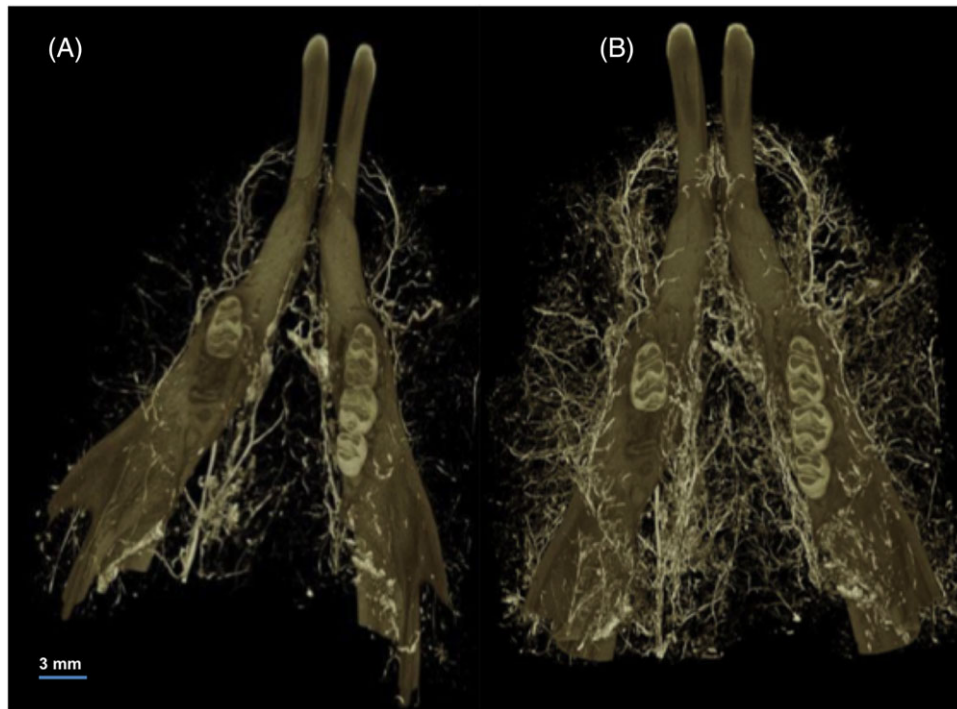


Fig. 3. Slices of a mandible after barium sulphate injection and acquisition with two micro-CT devices: the SIV1076 on the left (A) at  $9\ \mu\text{m}$  and the S1272 at  $6\ \mu\text{m}$  on the right (B) (2016\*2016).

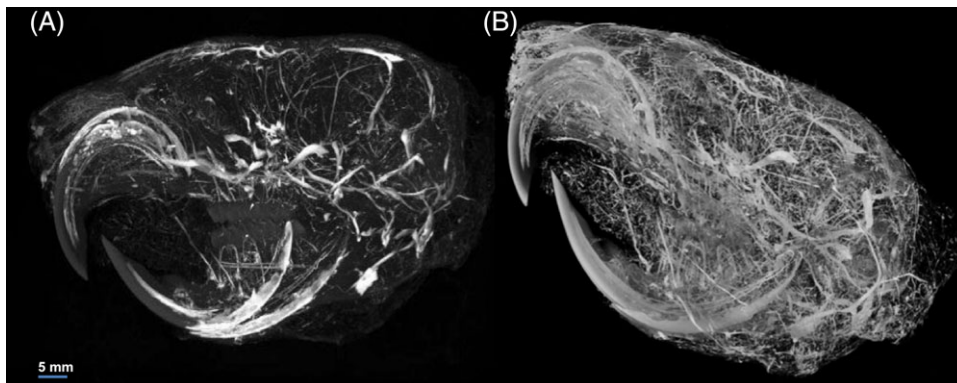
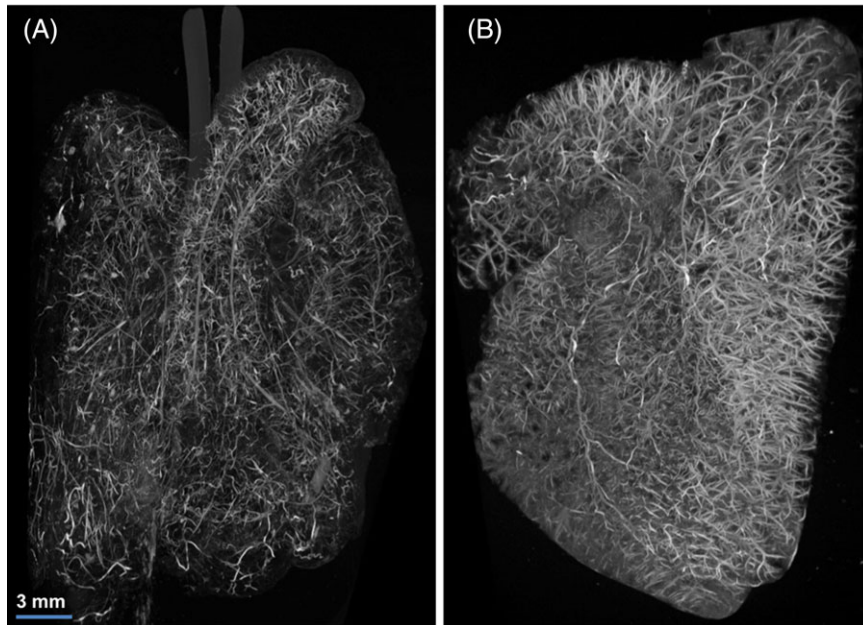


Fig. 4. Slices of a head after barium sulphate injection and acquisition with two micro-CT devices: the SIV1076 on the left (A) at  $9\ \mu\text{m}$  and the S1272 at  $6\ \mu\text{m}$  on the right (B) (3840\*3840).

study bone microarchitecture has been described in detail (Parfitt *et al.*, 1987; Guggenbuhl *et al.*, 2006; Brandi, 2009; Bouxsein *et al.*, 2010) and is considered a good tool to quantify bone microarchitecture. In 1987, Parfitt *et al.* (Parfitt *et al.*, 1987) standardized the symbols and units of the different bone microarchitecture parameters. Recently, other authors have studied vascular microarchitecture parameters, extrapolated from bone microarchitecture parameters (Bolland *et al.*, 2008; Jia *et al.*, 2010; Langer *et al.*, 2011; Prisby *et al.*, 2011; Roche *et al.*, 2012) using radio-opaque contrast agent. To calculate the vascular microarchitecture parameters, the vascular tree should be visible almost in its entirety. Two micro-CT

devices, an In Vivo Skyscan 1076 and a Skyscan 1272, were used for the same samples, at different or same resolution. Due to the progress in the X-ray source and camera techniques, the results obtained with the new S1272 micro-CT show better clarity and accuracy in terms of vessel quantity and details. Nearly all the vascular network was visible and identifiable. The results for soft tissues and organs were very good and reproducible (numerous tests of injection and acquisition were done, data not shown). Difficulty was experienced for the bone vascular network, all the soft tissues were easily injected; but sometimes the bone vasculature was not entirely perfused, due to the heterogeneous bone vascular network



**Fig. 5.** Mandible and tongue on the left (A) and liver on the right (B), after barium sulphate injection and acquisition with 1272 micro-CT at  $6\ \mu\text{m}$  (2016\*2016 for the mandible, 5664\*5664 for the liver).

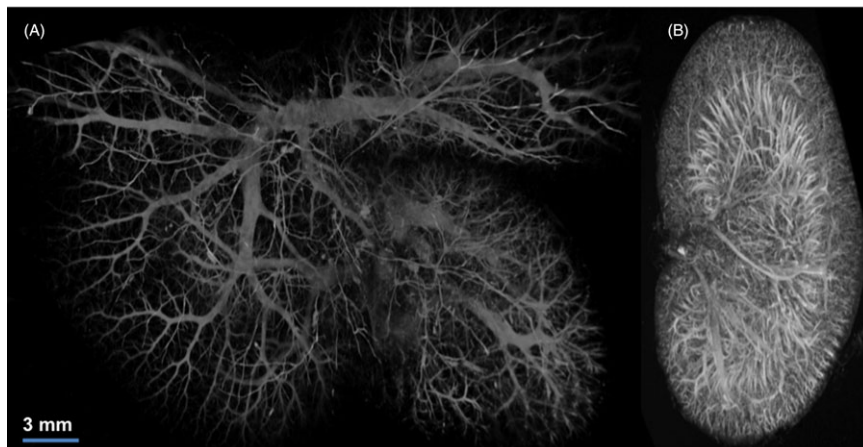


**Fig. 6.** Lung (A) and kidney (B) after barium sulphate injection and acquisition with 1272 micro-CT at  $6\ \mu\text{m}$  (5664\*5664 for the lung, 2016\*2016 for the kidney).

within an individual or between individuals (Jia *et al.*, 2010; Roche *et al.*, 2012). The protocol of contrast agent injection was not changed; only the improvements of the micro-CT device allow highlighting the entire vascular tree.

Thresholding is an important part of highlighting vessels after micro-CT acquisition to clearly distinguish vessels and bone. Alternative image processing methods exist. Clearly separating the vessels from the bone is important for a good estimation of the vascular and bone microarchitecture parameters. Several studies have reported different injection protocols and acquisition parameters, which prevents us from comparing the results. The results obtained with

this new micro-CT enabled the calculation of vascular microarchitecture parameters, although a computer with high processing speed is required.

Synchrotron-CT is considered the gold standard both for studying both 3-D bone microarchitecture and vascularization (Eppel *et al.*, 2009; Langer *et al.*, 2009; Chien *et al.*, 2010; Jia *et al.*, 2010; Lu *et al.*, 2010; Peyrin *et al.*, 2010; Roche *et al.*, 2012; Matsumoto *et al.*, 2013; Holme *et al.*, 2014; Neldam & Pinholt, 2014). Using this S1272 micro-CT, images are highly similar to those obtained with the synchrotron, for example in term of number and details of vessels. This 'desktop' micro-CT is therefore a good alternative to the synchrotron due to the



Fig. 7. 3-D volumes of a rat's organs after barium sulphate injection and 1272 micro-CT acquisition, at  $6\ \mu\text{m}$ . From top to bottom: head; larynx; heart; front legs; lungs; kidneys, liver and spleen, in the same line; femurs; tibias and back legs.

easier access, lower cost and the lower acquisition time. This injection protocol and the good results with this new micro-CT allow us to consider studying tissue neovascularization for pathological conditions such as cancer or metastasis and vascular engineering strategies with growth factors or cytokines.

## Conclusion

This paper presents images of hard and soft tissues after contrast agent injection in the bloodstream and acquisition with micro-CT. Images of vascularization of all the organs obtained with the Skyscan 1272 micro-CT are clearly defined with accuracy and clarity. The barium sulphate injection technique allows good images and these results open up possibilities in detection and characterization of 3-D vasculature, allowing us to study neovascularization and vascular engineering strategies. Prospects for future studies can now be extended to quantitative analysis for both soft and hard tissues and for connections between their vasculatures. For bone, interesting perspectives are expected in terms of understanding vascularization in healing or pathological situations, such as irradiation, or to extend knowledge of bone vascularization, given that the samples do not have to be decalcified when barium sulphate is used as contrast agent.

## Acknowledgements

This study was supported by grants from 'La Ligue Contre Le Cancer' foundation, committees 'Pays de La Loire' and 'Côtes d'Armor'. We thank Séverine Battaglia of LRPO for using In Vivo Skyscan 1076 and LBTO for learning the contrast agent injection technique.

## References

- Bentley, M.D., Ortiz, M.C., Ritman, E.L. & Romero, J.C. (2002). The use of microcomputed tomography to study microvasculature in small rodents. *Am. J. Physiol. - Regul. Integr. Comp. Physiol.* **282**, R1267–R1279.
- Bolland, B.J.R.F., Kanczler, J.M., Dunlop, D.G. & Oreffo, R.O.C. (2008). Development of in vivo  $\mu$ CT evaluation of neovascularisation in tissue engineered bone constructs. *Bone* **43**, 195–202.
- Bouxsein, M.L., Boyd, S.K., Christiansen, B.A., Guldborg, R.E., Jepsen, K.J. & Müller, R. (2010). Guidelines for assessment of bone microstructure in rodents using micro-computed tomography. *J. Bone Miner. Res.* **25**, 1468–1486.
- Brandi, M.L. (2009). Microarchitecture, the key to bone quality. *Rheumatology* **48**, iv3–iv8.
- Carano, R.A. & Filvaroff, E.H. (2003). Angiogenesis and bone repair. *Drug Discov. Today* **8**, 980–989.
- Chien, C.-C., Wang, C.H., Wang, C.L., et al. (2010). Synchrotron microangiography studies of angiogenesis in mice with microemulsions and gold nanoparticles. *Anal. Bioanal. Chem.* **397**, 2109–2116.
- Duvall, C.L., Taylor, W.R., Weiss, D. & Guldborg, R.E. (2004). Quantitative microcomputed tomography analysis of collateral vessel development after ischemic injury. *Am. J. Physiol. - Heart Circ. Physiol.* **287**, H302–H310.
- Eppel, G.A., Jacono, D.L., Shirai, M., Umetani, K., Evans, R.G. & Pearson, J.T. (2009). Contrast angiography of the rat renal microcirculation in vivo using synchrotron radiation. *Am. J. Physiol. Renal Physiol.* **296**, F1023–1031.
- Grabherr, S., Djonov, V., Yen, K., Thali, M.J. & Dirnhofer, R. (2007). Postmortem angiography: review of former and current methods. *Am. J. Roentgenol.* **188**, 832–838.
- Guggenbuhl, P., Bodic, F., Hamel, L., Baslé, M.F. & Chappard, D. (2006). Texture analysis of X-ray radiographs of iliac bone is correlated with bone micro-CT. *Osteoporos. Int.* **17**, 447–454.
- Hallouard, F., Anton, N., Choquet, P., Constantinesco, A. & Vandamme, T. (2010). Iodinated blood pool contrast media for preclinical X-ray imaging applications – A review. *Biomaterials* **31**, 6249–6268.
- Holme, M.N., Schulz, G., Deyhle, H., et al. (2014). Complementary X-ray tomography techniques for histology-validated 3D imaging of soft and hard tissues using plaque-containing blood vessels as examples. *Nat. Protoc.* **9**, 1401–1415.
- Jia, F., Françoise, P., Malaval, L., Laurence, V. & Marie-Hélène, L.-P. (2010). Imaging and Quantitative Assessment of Long Bone Vascularization in the Adult Rat Using Microcomputed Tomography. *Anat. Rec. Adv. Integr. Anat. Evol. Biol.* **293**, 215–224.
- Langer, M., Prisby, R., Peter, Z., Boistel, R., Lafage-Proust, M.-H. & Peyrin, F. (2009). Quantitative investigation of bone microvascularization from 3D synchrotron micro-computed tomography in a rat model. *Conf. Proc. IEEE Eng. Med. Biol. Soc.* **2009**, 1004–1007.
- Langer, M., Prisby, R., Peter, Z., Guignandon, A., Lafage-Proust, M.-H. & Peyrin, F. (2011). Simultaneous 3D imaging of bone and vessel microstructure in a rat model. *IEEE Trans. Nucl. Sci.* **58**, 139–145.
- Lu, W., Dong, Z., Liu, Z., et al. (2010). Detection of microvasculature in rat hind limb using synchrotron radiation. *J. Surg. Res.* **164**, e193–e199.
- Marxen, M., Thornton, M.M., Chiarot, C.B., Klement, G., Koprivnikar, J., Sled, J.G. & Henkelman, R.M. (2004). MicroCT scanner performance and considerations for vascular specimen imaging. *Med. Phys.* **31**, 305–313.
- Matsumoto, T., Goto, D. & Sato, S. (2013). Subtraction micro-computed tomography of angiogenesis and osteogenesis during bone repair using synchrotron radiation with a novel contrast agent. *Lab. Investig. J. Tech. Methods Pathol.* **93**, 1054–1063.
- Mondy, W.L., Cameron, D., Timmermans, J.-P., De Clerck, N., Sasov, A., Casteleyn, C. & Piegl, L.A. (2009a). Computer-aided design of microvasculature systems for use in vascular scaffold production. *Biofabrication*; **1**(3), 035002.
- Mondy, W.L., Cameron, D., Timmermans, J.-P., De Clerck, N., Sasov, A., Casteleyn, C. & Piegl, L.A. (2009b). Micro-CT of corrosion casts for use in the computer-aided design of microvasculature. *Tissue Eng. Part C Methods* **15**, 729–738.
- Moore, D.C., Leblanc, C.W., Müller, R., Crisco, J.J. & Ehrlich, M.G. (2003). Physiologic weight-bearing increases new vessel formation during distraction osteogenesis: A micro-tomographic imaging study. *J. Orthop. Res.* **21**, 489–496.
- Neldam, C.A. & Pinholt, E.M. (2014). Synchrotron  $\mu$ CT imaging of bone, titanium implants and bone substitutes—a systematic review of the literature. *J. Cranio-Maxillofac. Surg.* **42**, 801–805.
- Nyangoga, H., Mercier, P., Libouban, H., Baslé, M.F. & Chappard, D. (2011). Three-dimensional characterization of the vascular bed in bone metastasis of the rat by microcomputed tomography (MicroCT). *PLoS ONE* **6**, e17336.

- Oses, P., Renault, M.-A., Chauvel, R., et al. (2009). Mapping 3-dimensional neovessel organization steps using micro-computed tomography in a murine model of hindlimb ischemia—brief report. *Arterioscler. Thromb. Vasc. Biol.* **29**, 2090–2092.
- Pabst, A.M., Ackermann, M., Wagner, W., Haberthür, D., Ziebart, T. & Kondering, M.A. (2014). Imaging angiogenesis: perspectives and opportunities in tumour research—A method display. *J. Cranio-Maxillofac. Surg.* **42**(6), 915–923.
- Parfitt, A.M., Drezner, M.K., Glorieux, F.H., Kanis, J.A., Malluche, H., Meunier, P.J., Ott, S.M. & Recker, R.R. (1987). Bone histomorphometry: standardization of nomenclature, symbols, and units: report of the asbmr histomorphometry nomenclature committee. *J. Bone Miner. Res.* **2**, 595–610.
- Peyrin, F., Attali, D., Chappard, C. & Benhamou, C.L. (2010). Local plate/rod descriptors of 3D trabecular bone micro-CT images from medial axis topologic analysis. *Med. Phys.* **37**, 4364–4376.
- Prisby, R., Guignandon, A., Vanden-Bossche, A., et al. (2011). Intermittent PTH(1–84) is osteoanabolic but not osteoangiogenic and relocates bone marrow blood vessels closer to bone-forming sites. *J. Bone Miner. Res.* **26**, 2583–2596.
- Roche, B., David, V., Vanden-Bossche, A., Peyrin, F., Malaval, L., Vico, L. & Lafage-Proust, M.-H. (2012). Structure and quantification of microvascularisation within mouse long bones: what and how should we measure? *Bone* **50**, 390–399.
- Roche, B., van den Bossche, A., Normand, M., Malaval, L., Vico, L. & Lafage-Proust, M.-H. (2013). Validated Doppler measurement of mouse bone blood perfusion — response to age or ovariectomy differs with genetic background. *Bone* **55**(2), 418–426.
- Saran, U., Gemini Piperni, S. & Chatterjee, S. (2014). Role of angiogenesis in bone repair. *Arch. Biochem. Biophys.* **561**:109–117.
- Schneider, P., Krucker, T., Meyer, E., et al. (2009). Simultaneous 3D visualization and quantification of murine bone and bone vasculature using micro-computed tomography and vascular replica, simultaneous 3D visualization and quantification of murine bone and bone vasculature using micro-computed tomography and vascular replica. *Microsc. Res. Tech. Microsc. Res. Tech.* **72**, 690–701.
- Young, S., Kretlow, J.D., Nguyen, C., Bashoura, A.G., Baggett, L.S., Jansen, J.A., Wong, M. & Mikos, A.G. (2008). Microcomputed tomography characterization of neovascularization in bone tissue engineering applications. *Tissue Eng. Part B Rev.* **14**, 295–306.